Landslides

most of the ⊕'s surface is not occupied by streams

Streams are ~~actually~~ the conveyer belts of sediment to ~~t~~ the oceans.

~~But how do soil & rock get into the streams?~~

Figure 3.23 from Holmes gives one an idea of relative proportions of stream bottom vs. bank erosion.

How do soil & rock get into streams?

- overland flow
- slope wash
- rill & gully incision

These are most important mechanisms on exposed soil — plowed fields, fresh volcanic ash, slopes after fires — man plays an important role here.

- rock & soil creep
- solifluction
- rock falls & avalanches
- landslides

↑ Particularly in rugged mountain regions with rapid erosion rates (Taiwan, Papua New Guinea, Himalaya, New Zealand) this is the most important erosion agent

Drainage Density, Channel Frequency

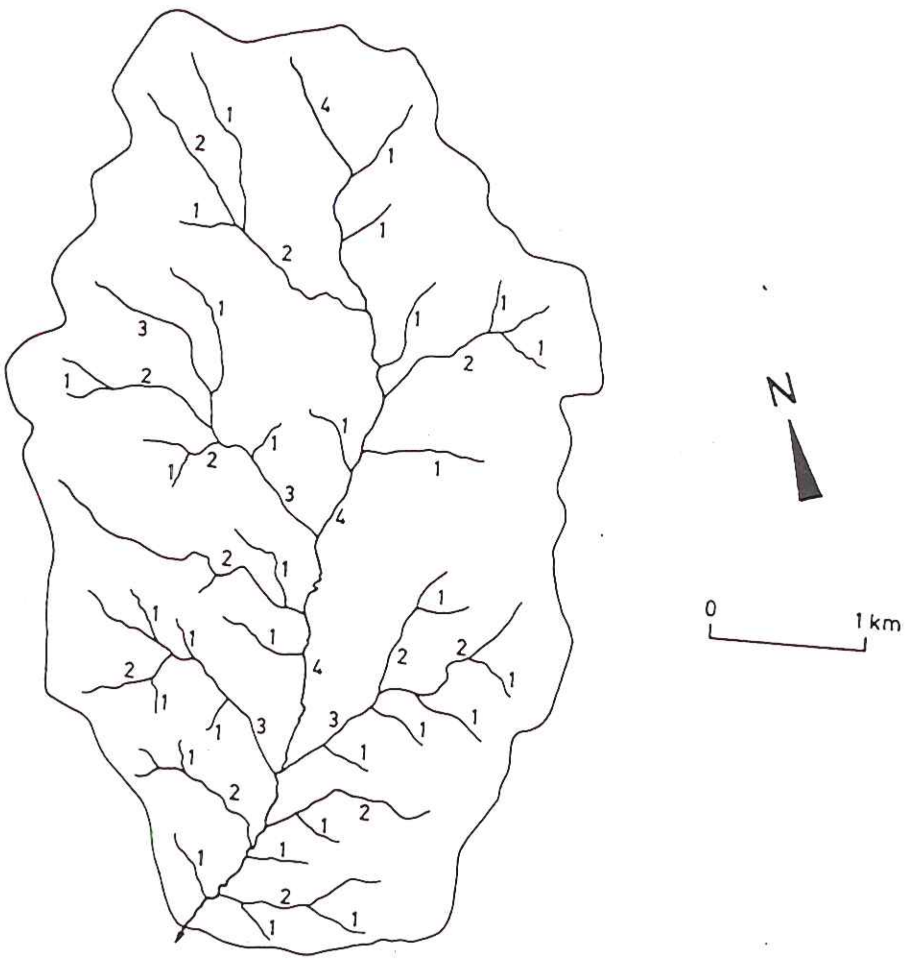

Fig. 6.6. Stream ordering after Horton. (In: Leopold et al. 1964)

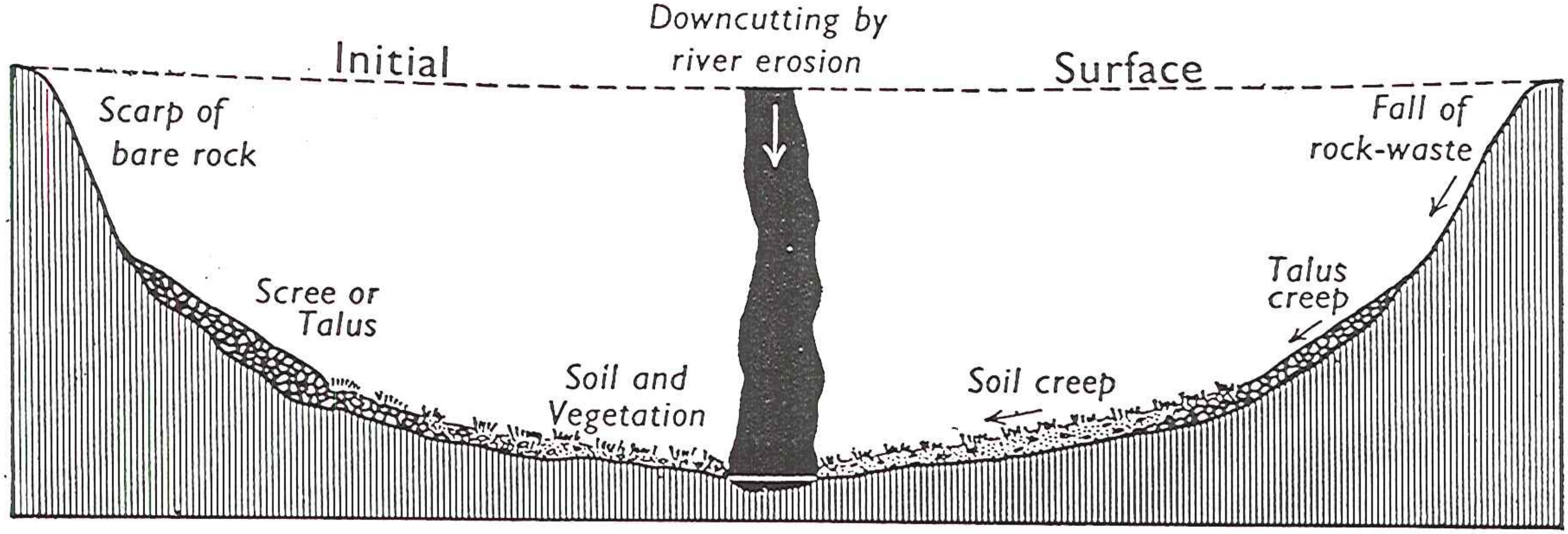

FIG. 323 Diagram illustrating the contrast between the amount of material eroded by a downcutting stream and that supplied to it by the processes that wear back the valley sides

Southern Alps New Zealand

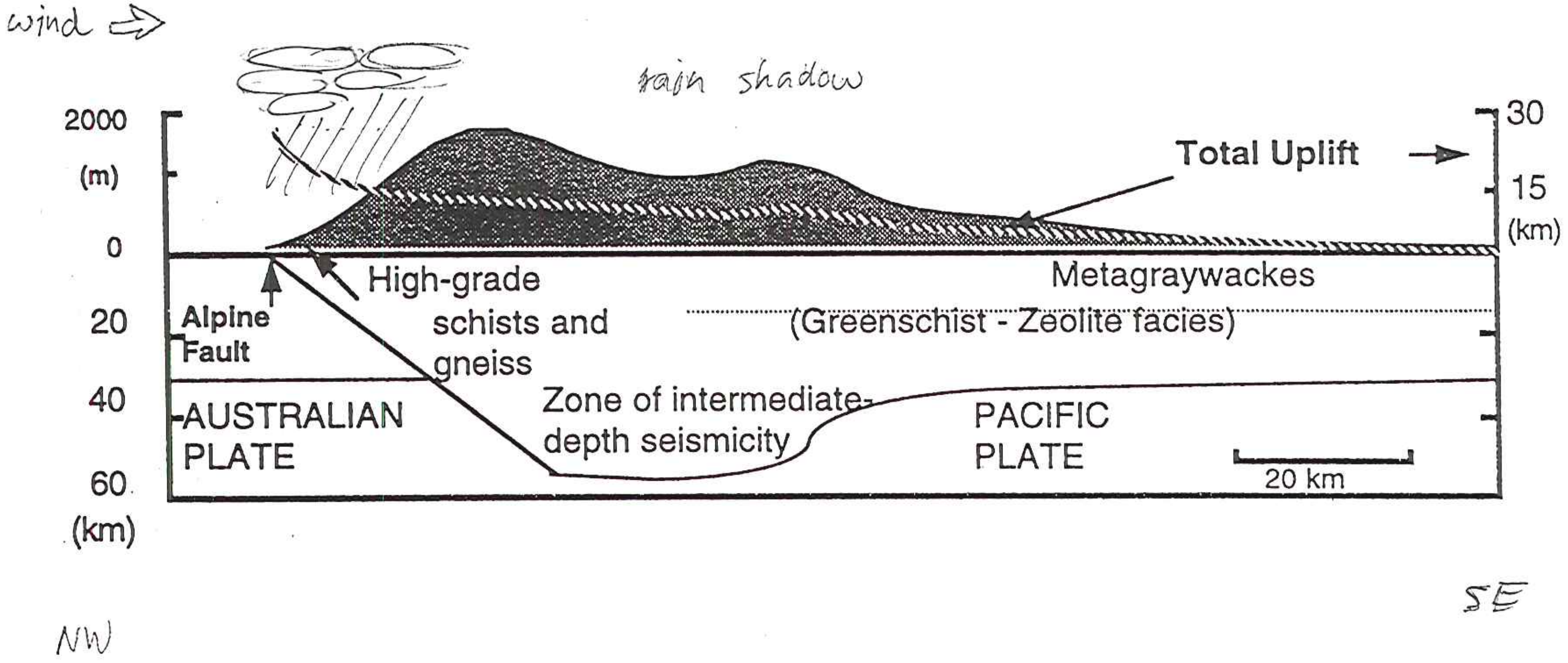

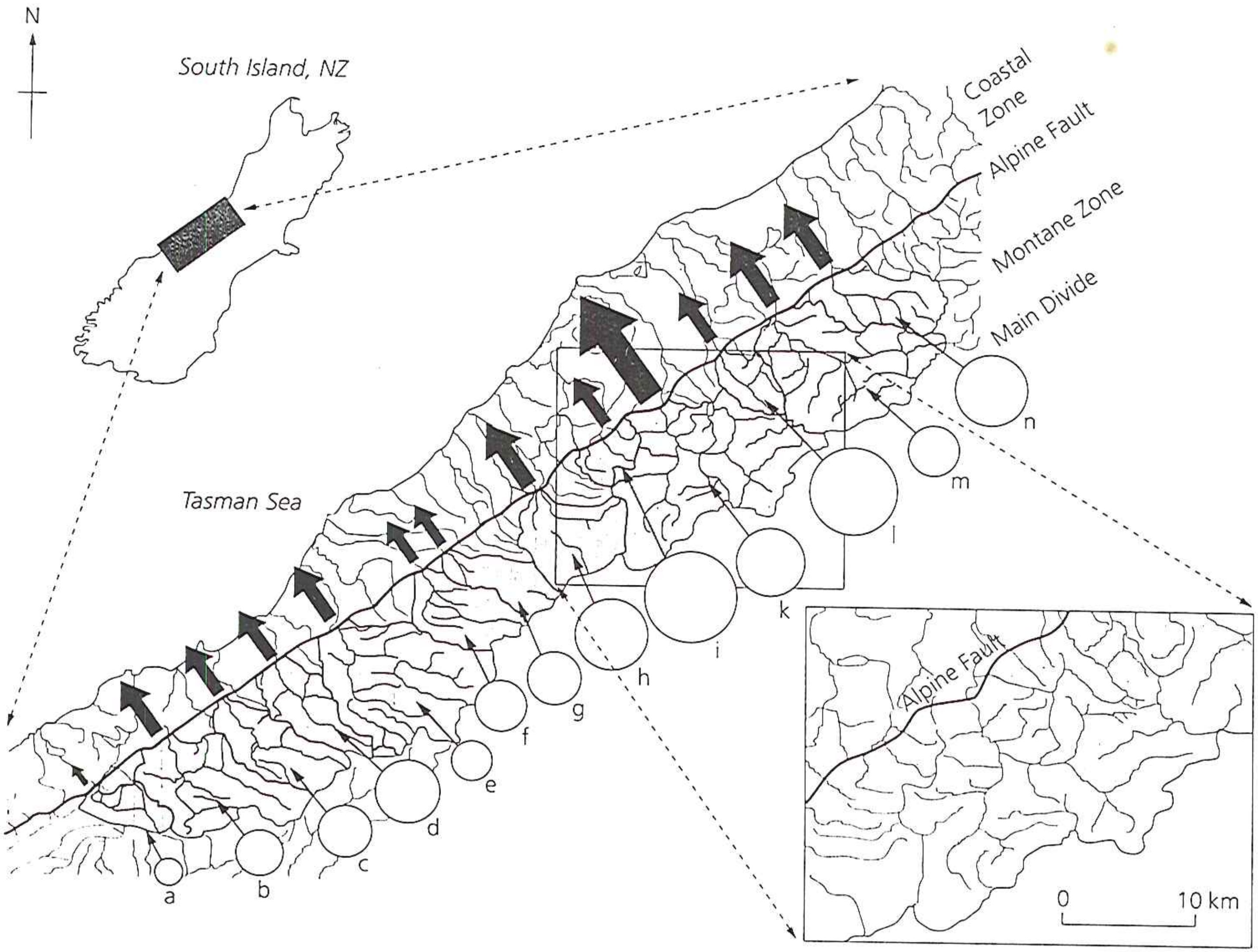

Fig. 3.18 The landslide efflux of mountainous hillslopes, Southern Alps, New Zealand, derived from the same dataset as in Fig. 3.17. Denudation rates of each of 13 catchments draining the western side of the Southern Alps are shown proportional to the areas of circles and vary from 1.8 mm y^{-1} in Moeraki catchment (a) to 18.1 mm y^{-1} in Waitangitaona (j) and Poerua (l) catchments. The sediment discharges are proportional to the size of arrows leaving the catchments, ranging from $1.2 \times 10^5 m^3 y^{-1}$ in Moeraki catchment (a) to $5.1 \times 10^6 m^3 y^{-1}$ in Whataroa catchment (k). After Hovius *et al.* 1997 [24].

Best study of this by Hovius & others

Southern Alps of New Zealand

Very steep mountains:

why is weather from W?
NZ south of 30°

$\dot{e}$ very high — even higher than Taiwan

Prevailing winds from west (Tasman Sea)
Drop all moisture on steep western flank

Studied series of aerial photos

2670 km^2 total study area

Measured sizes of all landslide scars:

$\frac{1}{200}$ $km^2 \le$ areas ≤ 1 km^2

size of a football field

Area is heavily vegetated (because lots of rain)

Could infer ages of scars from extent of revegetation

Typical scar elliptical in shape:

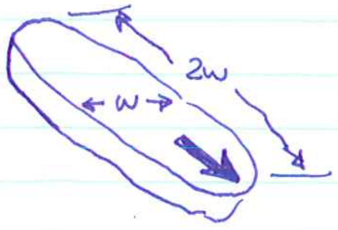

twice as wide as long

area $A = \frac{\pi}{2} w^2 = 1.6 \, w^2$

w = width

On-site observation showed that typical scar was thin:

thickness

$$t = \underbrace{(0.04 \pm 0.02)}_{\text{call this } \varepsilon} \sqrt{A}$$

Volume of material in a typical slide

$$\boxed{\begin{aligned} V &= \varepsilon A^{3/2} \\ V &= (0.04 \pm 0.02) A^{3/2} \end{aligned}}$$

They found a total of ~ 5000 slides between 1948 & 1986

About 60 years of data

Individual slides shown as black smudges in inset blowup map Fig. 1

Plotted cumulative number versus slide area (log-log plot)

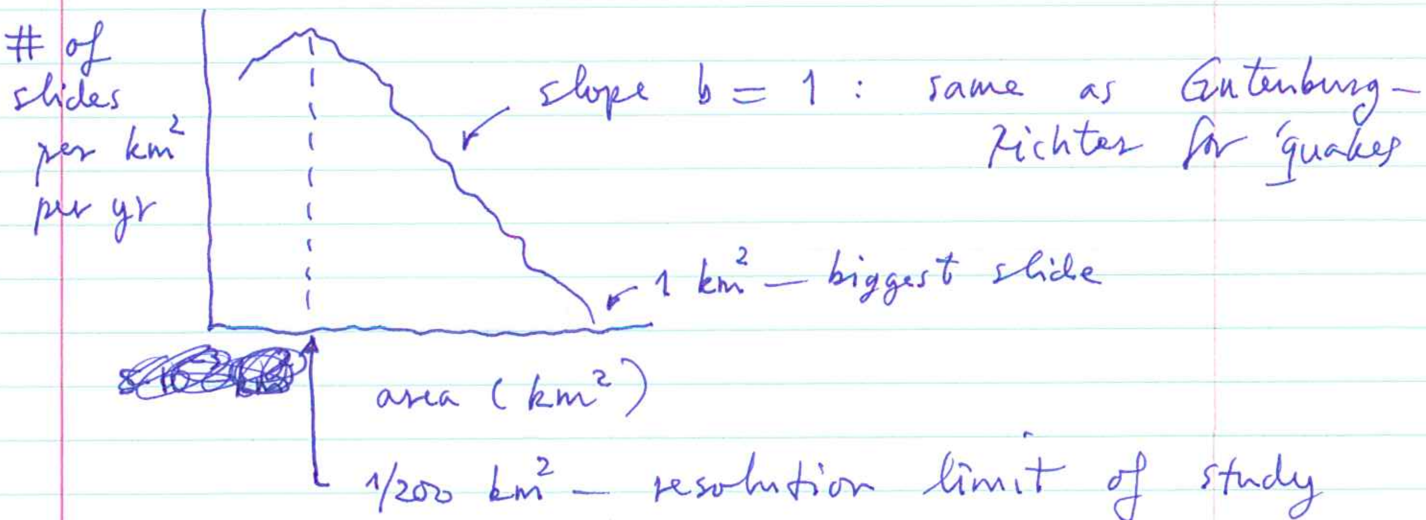

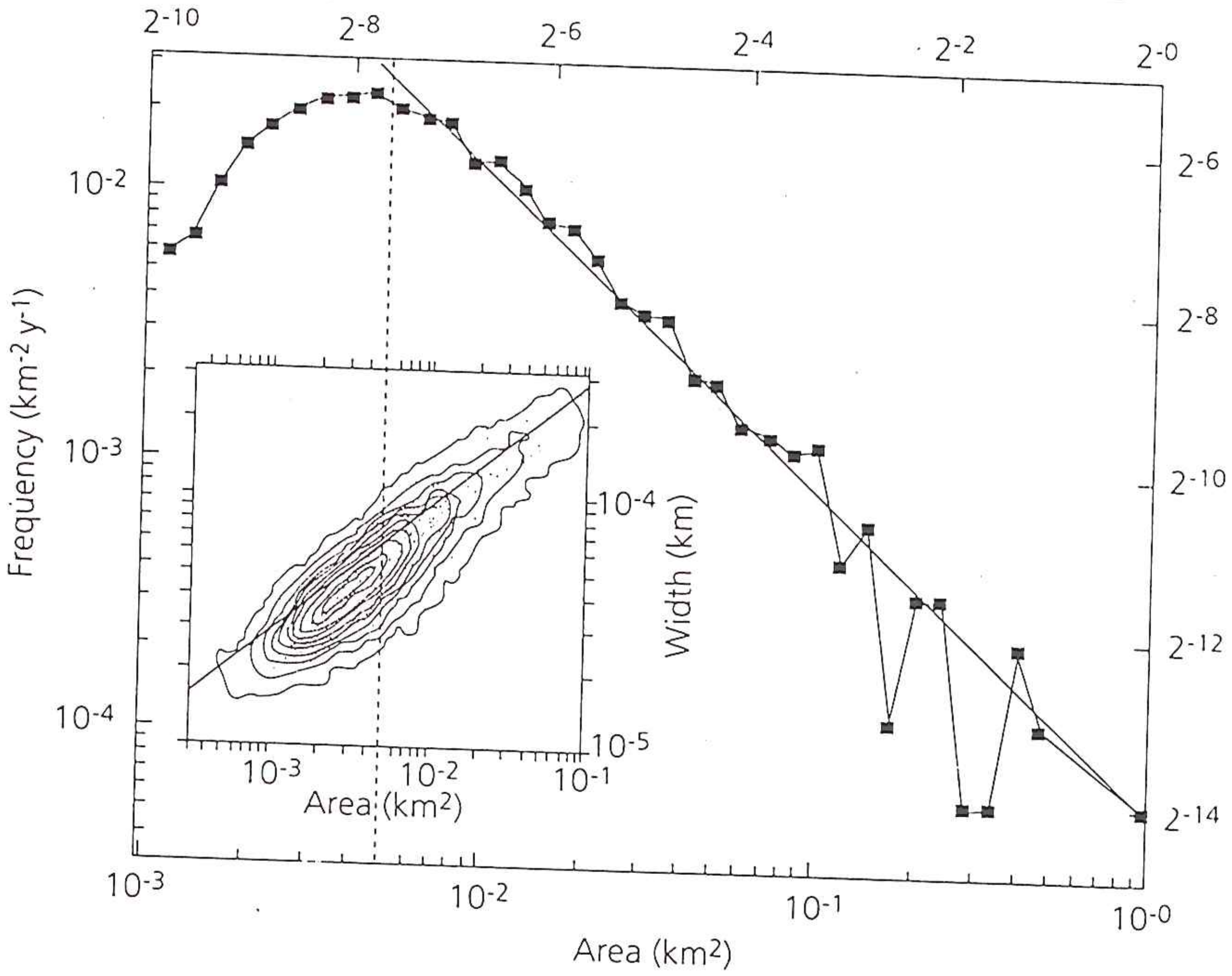

Fig. 3.17 The power law magnitude–frequency distribution of landslides in the Southern Alps (New Zealand), derived from mapping 4984 landslide events east of the Alpine fault which have occurred over the last 60 years. The area to the left of the vertical dashed line is below mapping resolution and should be ignored. The inset graph shows the relationship between the landslide area and the width of the best-fit ellipse, giving information on the plan-view aspect of the landslide scars. After Hovius *et al.* (1997) [24].

aA^{-b} with $b = 1$

N (with area $\leq A$) $= a A^{-1}$

$a = 5.4 \cdot 10^{-5}$ per km^2 per year

↑ # per km^2 per year

recall study area 2670 km^2

study interval 60 yrs

recall this is the cumulative distribution

$N =$ number with area $\leq A$

$$\boxed{\begin{aligned} \log_{10} N &= a - bA \\ a &= 5.4 \cdot 10^{-5}\ \text{km}^{-2}\ \text{yr}^{-1} \\ b &= 1 \end{aligned}}$$

Calculate erosion rate by adding up the volume of all these slides — analogous to computing total energy released by all 'quakes

$A_{\text{middle of range}}$ in this range $= \frac{1}{2}(1 + 1/4) = 5/8$ km^2

area range (km^2)	# per km^2 per year in this range	total # in 2670 km^2 study area per year	total slide volume per km^2 per year from slides in this range [# per km^2 per year $\times\ \varepsilon A_{\text{middle of range}}^{3/2}$]
$1 \leq A \leq 1/4$	3a	0.5	$15/8\ \varepsilon a \equiv V_{biggies}$
$1/4 \leq A \leq 1/16$	12a	1.8	$\frac{1}{2} V_{biggies}$
$1/16 \leq A \leq 1/64$	48a	7.3	$\frac{1}{4} V_{biggies}$
$1/64 \leq A \leq 1/256$	132a	29	$1/8\ V_{biggies}$
$1/256 \leq A \leq 1/1024$	768 a	117	$1/16\ V_{biggies}$
			$\vdots$

adds to ~9000 when multiplied by 60 year time period — actually saw only 5000 — cutoff at small size

So... the total volume of slide material per km² per year is...

$$\boxed{\begin{aligned} V_{total} &= \left(1 + \frac{1}{2} + \frac{1}{4} + \frac{1}{8} + \frac{1}{16} + \cdots\right) V_{biggies} \\ &= 2\,V_{biggies} \end{aligned}}$$

The landslide flux is dominated by the biggest landslides — just like energy release by earthquakes

This is the erosion rate due to landsliding — volume removed per km² per yr

$$\frac{km^3}{km^2\,yr} = \frac{km}{yr}$$

$$\begin{aligned} \dot{e} = 2V_{biggies} &= \frac{15}{4}\,\varepsilon\, a \\ &= \frac{15}{4}\,(0.04 \pm 0.02)(5.4 \cdot 10^{-5}) \\ &= (8 \pm 4) \cdot 10^{-6}\ km/yr \end{aligned}$$

$$\boxed{\begin{aligned} \dot{e}_{landsliding} &= 8 \pm 4\ km/Myr \\ & \quad 80 \times \langle \dot{e} \rangle_{\oplus} \end{aligned}}$$

The formal uncertainty due only to uncertainty in slide thickness and therefore volume.

area range (km^2)	# per km^2 per year in this range	total # in 2670 km^2 study area per year	per km^2 per year from slides in this range [# per km^2 per year $\times \varepsilon A_{\text{middle of range}}^{3/2}$)
$1 \le A \le 1/4$	$3a$	0.5	$15/8\, \varepsilon a \equiv V_{\text{biggies}}$
$1/4 \le A \le 1/16$	$12a$	1.8	$\frac{1}{2} V_{\text{biggies}}$
$1/16 \le A \le 1/64$	$48a$	7.3	$\frac{1}{4} V_{\text{biggies}}$
$1/64 \le A \le 1/256$	$132a$	29	$1/8\, V_{\text{biggies}}$
$1/256 \le A \le 1/1024$	$768a$	117	$1/16\, V_{\text{biggies}}$
			$\vdots$

The total volume of slide material per km^2 per yr is

$$\dot{e}_{\text{landsliding}} = V_{\text{total}} = \left(1+\frac{1}{2}+\frac{1}{4}+\frac{1}{8}+\cdots\right) V_{\text{biggies}} = 2 V_{\text{biggies}}$$

$$= \frac{15}{4}\varepsilon a = \frac{15}{4}(0.04 \pm 0.02)(5.4 \cdot 10^{-5})$$

$$= (8 \pm 4) \cdot 10^{-6}\ km/yr$$

$$\boxed{\dot{e}_{\text{landsliding}} = 8 \pm 4\ km/Myr}$$

The dominance of the biggest slides gives rise to additional uncertainty. Was the 60-year interval long enough to capture the biggest slide

Note jitter in histogram for large slides — there are not very many of these in the database.

Nevertheless, despite these uncertainties, value agrees very well with erosion rates measured by gaging of streams running into the Tasman Sea:

highest known $\dot{e}$ in world

$$\boxed{5\ \text{km/Myr} \le \dot{e}_{\text{streamloads}} \le 11\ \text{km/Myr}}$$

There is also fair geographic agreement where the landslide flux (size of circle ⊛) is large, the stream discharge (size of arrow ↖) is large too.

Conclusion — the rapid erosion rate in Southern Alps of New Zealand is dominated by landslide-derived material

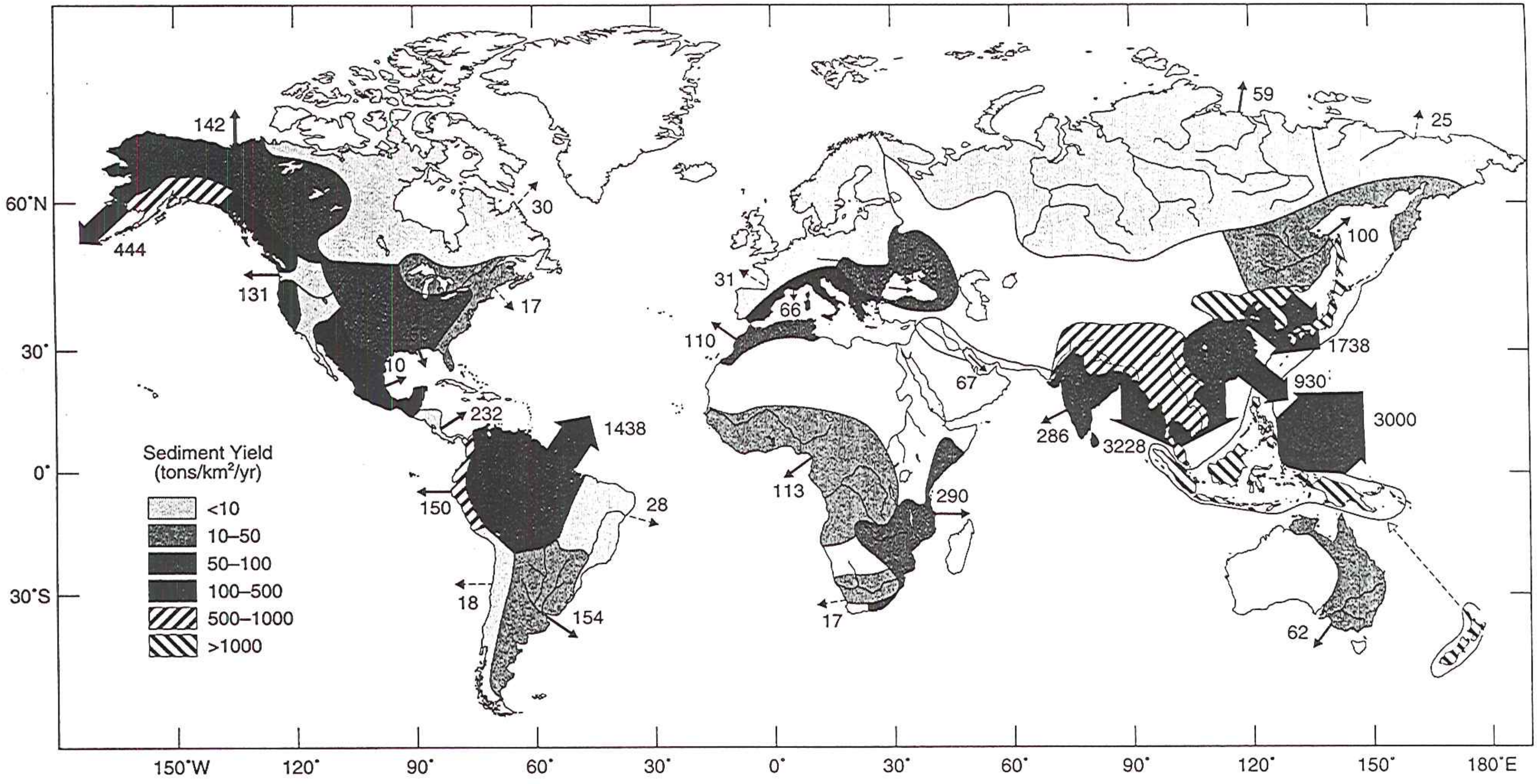

Figure 5.1. Discharge of suspended sediment from world drainage basins (in 10^6 tons/yr) as indicated by arrows. Sediment yield (tons/km^2/yr) for various drainage basins is also shown by appropriate pattern (see legend). Open pattern indicates essentially no sediment discharges to the oceans. [After J. D. Milliman and R. H. Meade. "World-Wide Delivery of River Sediment to the Oceans," *Journal of Geology* 91(1): 16. Copyright © 1983 by The University of Chicago Press, reprinted by permission of the publisher.]

100 tons /km^2 /yr = 0.04 km/Myr erosion rate

landsliding controls erosion
in all ▨ areas

Dominant control on $\dot{e}$ in high-erosion high-relief areas is rate of landsliding.

But what controls the rate of landsliding?

Sort of a chicken-and-egg problem:

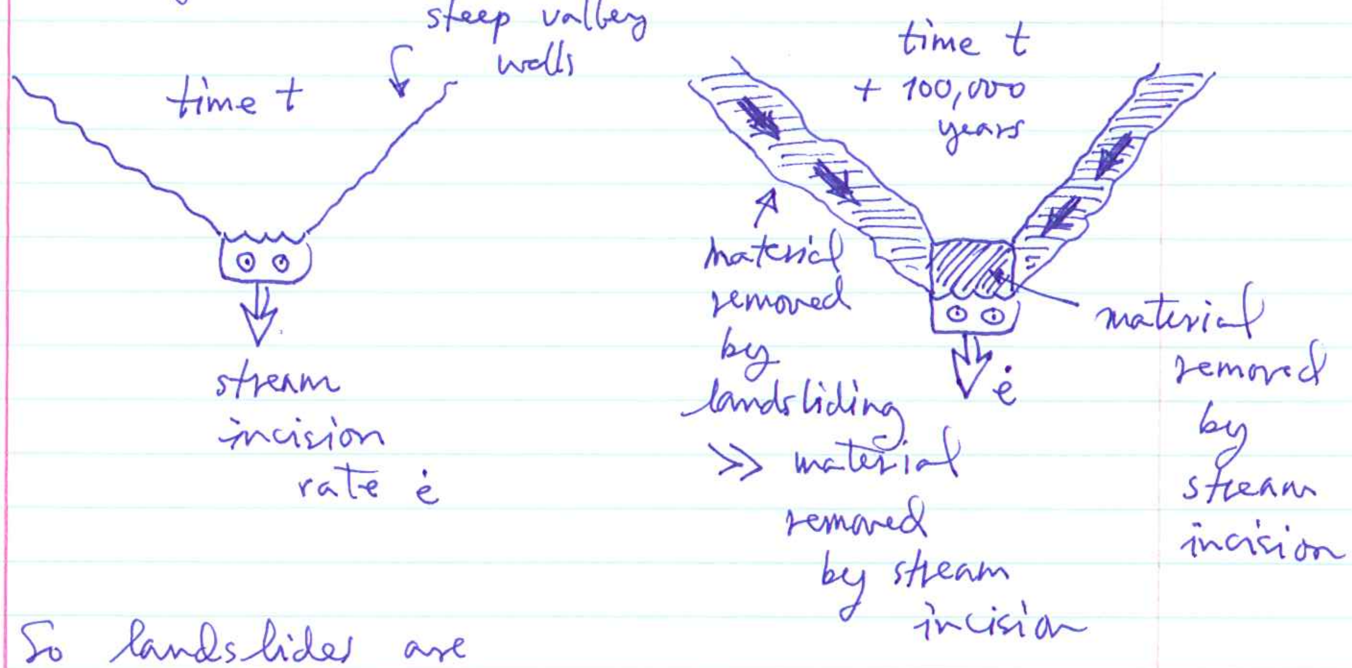

So landslides are the dominant source of eroded sediments

But rate of stream incision affects the rate of landsliding.

Note that I have sketched the situation so that the valley walls — which are constructed by continued landsliding — have a ~~[illegible] (constant)~~ constant (critical) slope.

Example — hillslope profiles from rapidly uplifting Santa Cruz Mtns in California Coast Range — slope angle ~ 26°

Ventura Basin, S. Calif.

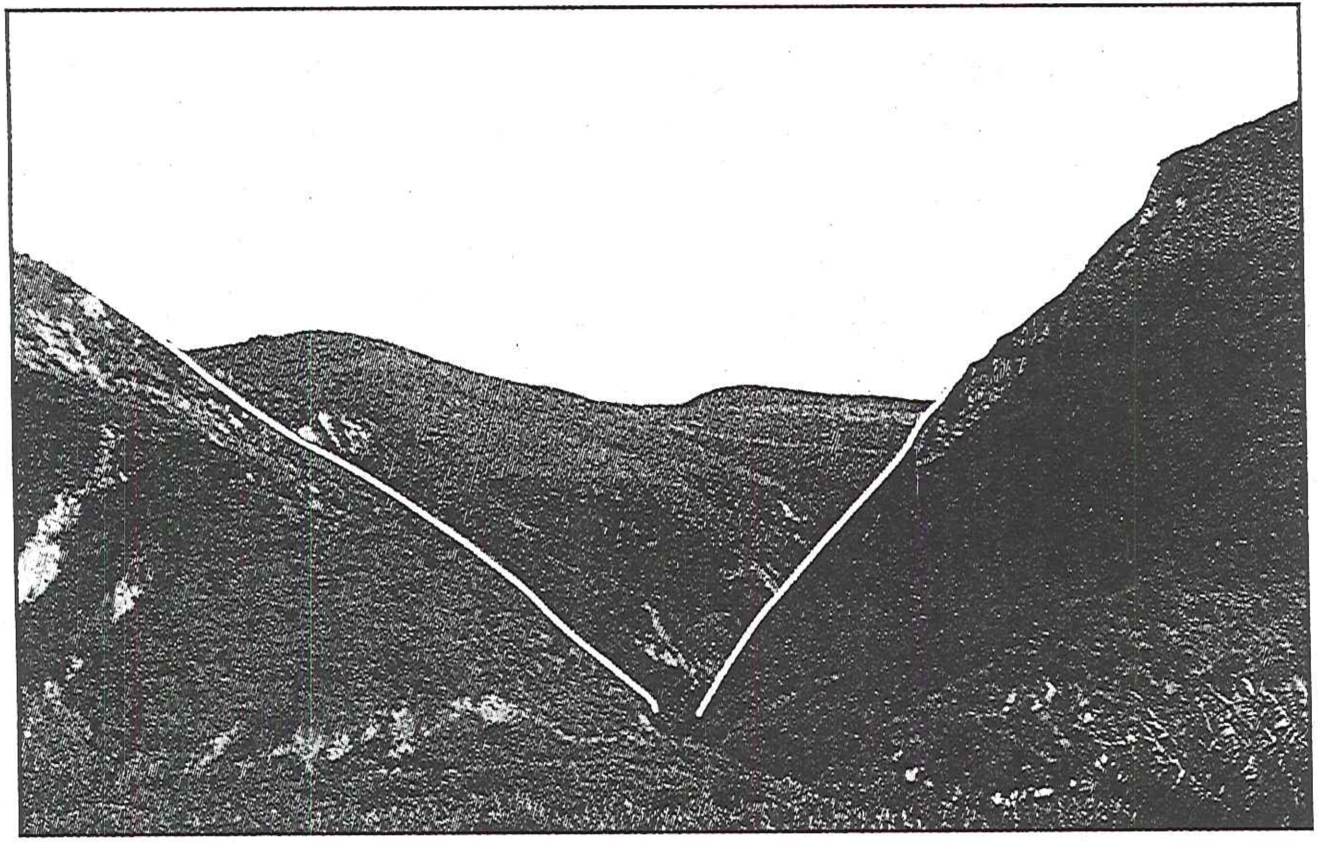

Figure 7. V-shaped valley of basin number 13 (Fig. 5), suggesting vertical erosion in response to uplift. Relief is ~150 m.

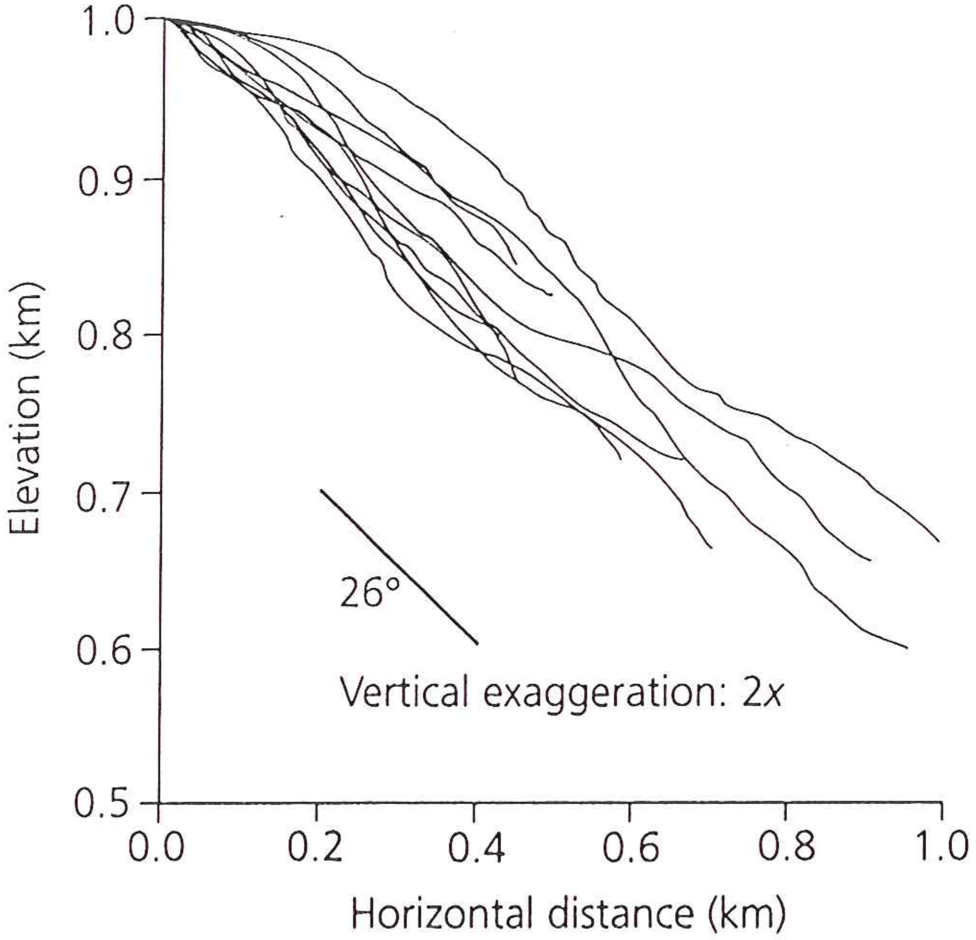

Fig. 3.21 Hillslope profiles from Santa Cruz Mountains. The long straight segments indicate that diffusion is overwhelmed by landsliding. The mean slope is about 26°. After Anderson (1994) [25].

What controls the slope angle of landslides?

We can analyze this problem by considering the sliding of an object down an inclined plane:

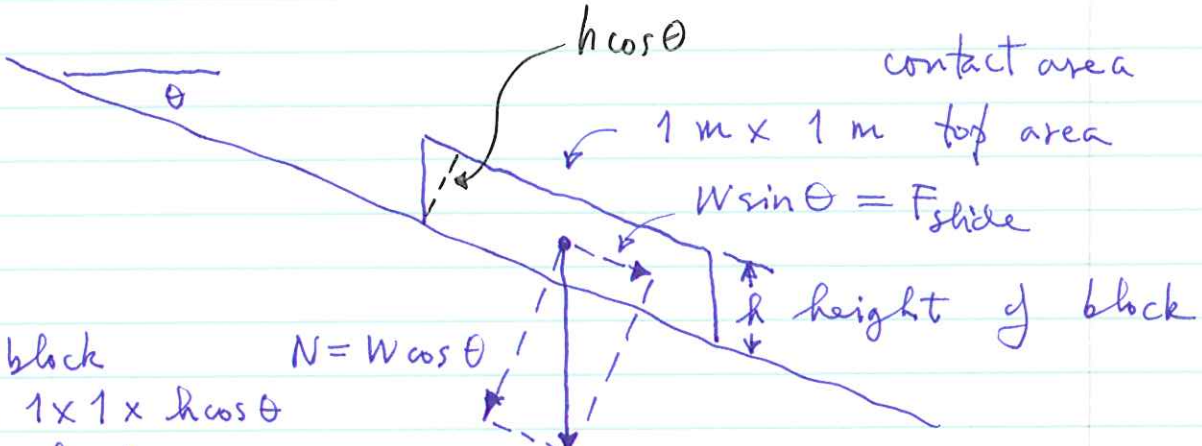

reason: block volume = 1 × 1 × h cos θ

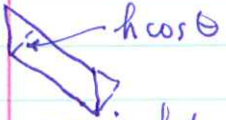

weight: $\boxed{W = \rho g h \cos\theta}$

Note: since we consider a 1 m × 1 m ~~[illegible]~~ block, these are forces per unit contact area

normal force: $\boxed{\begin{array}{l} W\cos\theta \\ N = W\cos\theta \end{array}}$

downslope force — acts to cause sliding: $W\sin\theta$

The block will slide when: $\boxed{F_{slide} = W\sin\theta}$

sliding force exceeds resistive force

Resistive force has two components

~~$F_{resist} = C + \mu W \cos\theta$~~

$$F_{resist} = C + \mu N = C + \mu W\cos\theta$$

cohesion (e.g. block may be glued to slide surface)

friction: proportional to normal force

$\boxed{\mu : \text{coefficient of friction}}$

NB — need to emphasize that F_{resist} is really a strength — the resistive force on the verge of sliding

The slide condition is

$$F_{slide} = F_{resist}$$

F_{resist} is present even when level:

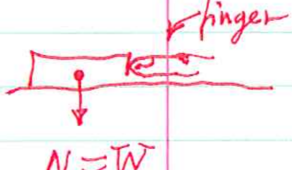

~~$\rho g h \sin\theta = C + \mu \rho g h \cos\theta$~~

$$W\sin\theta = C + \mu W\cos\theta$$

$$\mu = \tan\theta + \frac{C}{W\cos\theta}$$

$$\boxed{\mu = \tan\theta + \frac{C}{\rho g h \cos^2\theta}}$$

Note — friction is independent of contact area!

(illustrate with marble block)

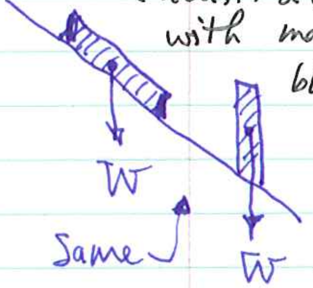

units:

μ – dimensionless

C – MPa

Relation between critical slope angle θ, coefficient of friction μ, and cohesion C.

Latter two are material properties.

~~The coefficient of friction is fairly independent of rock type~~

Example — dry sand

$\mu \cong 0.6 - 0.7$

$C = 0$ MPa

$$\boxed{\theta = \arctan\mu \approx 30^\circ - 35^\circ}$$

~~Examples~~:

↑ this is known as the angle of repose

Hourglass:

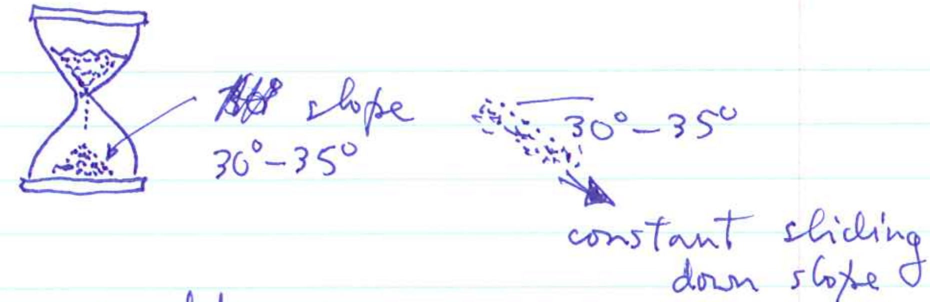

Lee face of a sanddune:

Scree slope:

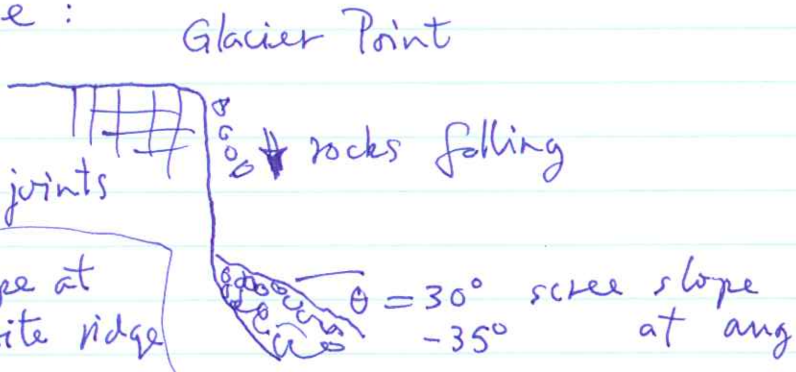

at angle of repose — as you know if you've ever tried to climb one

e.g., scree slope at base of quartzite ridge at Water Gap

Volkswagen sized boulders

In fact $\mu \approx 0.6$ is often taken to be the nominal coefficient of friction of common silicate rocks

Byerlee's law: so-called "maximum" friction $\mu = 0.85$ — essentially independent of rock type

μ	θ	
0.85	40°	
0.6	31° — nominal	
0.4	22°	clay-rich
0.2	11°	

Clay-rich horizons can have lower coefficients of friction: $\mu \approx 0.2 - 0.4$

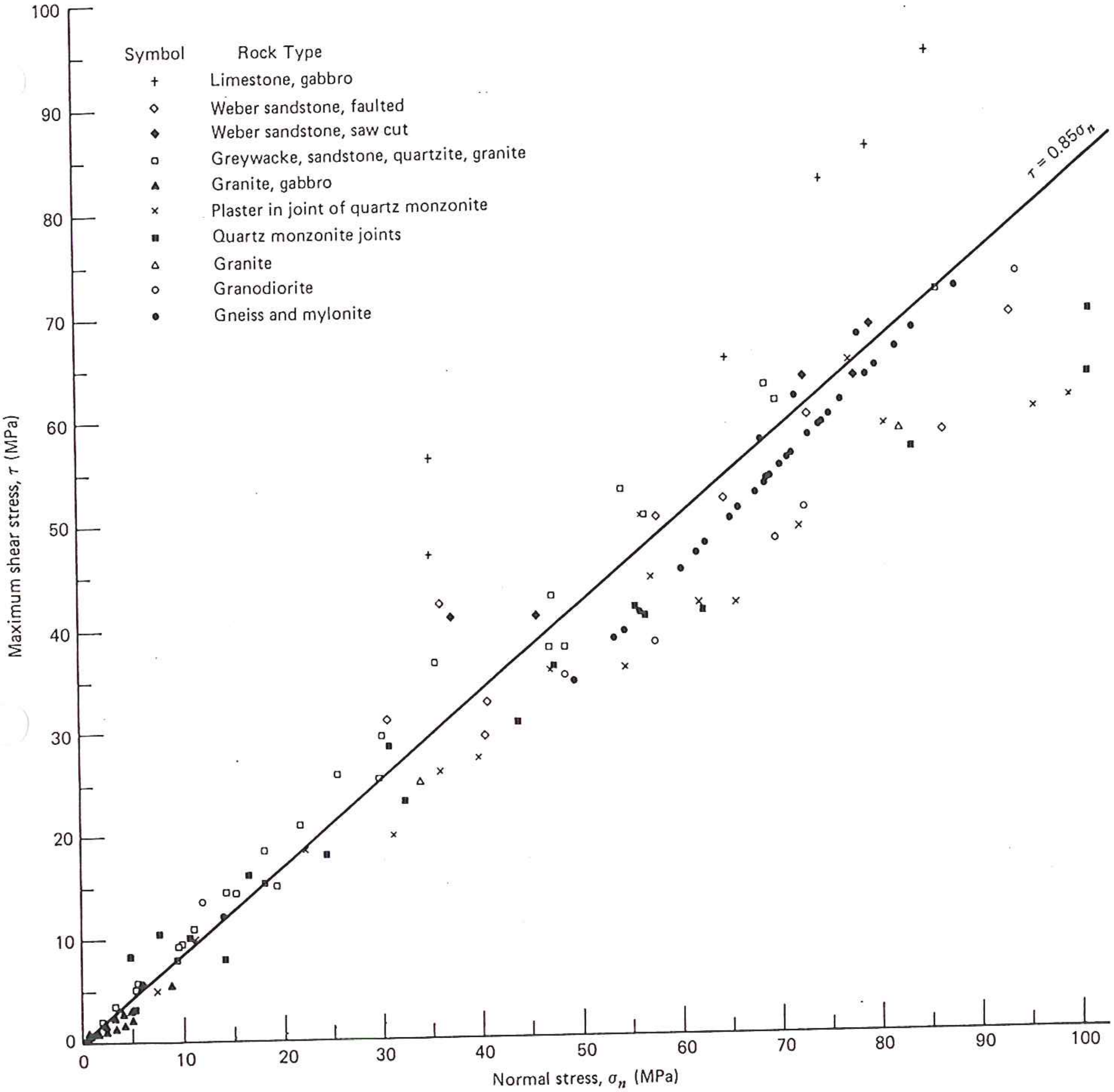

Figure 8-6 Maximum shear stress to initiate sliding as a function of normal stress for a variety of rock types. The linear fit defines a maximum coefficient of static friction max f_s equal to 0.85. Data from J. D. Byerlee, Friction of rocks, in *Experimental Studies of Rock Friction with Application to Earthquake Prediction*, ed. J. F. Evernden, pp. 55–77, U.S. Geological Survey, Menlo Park, Calif., 1977.

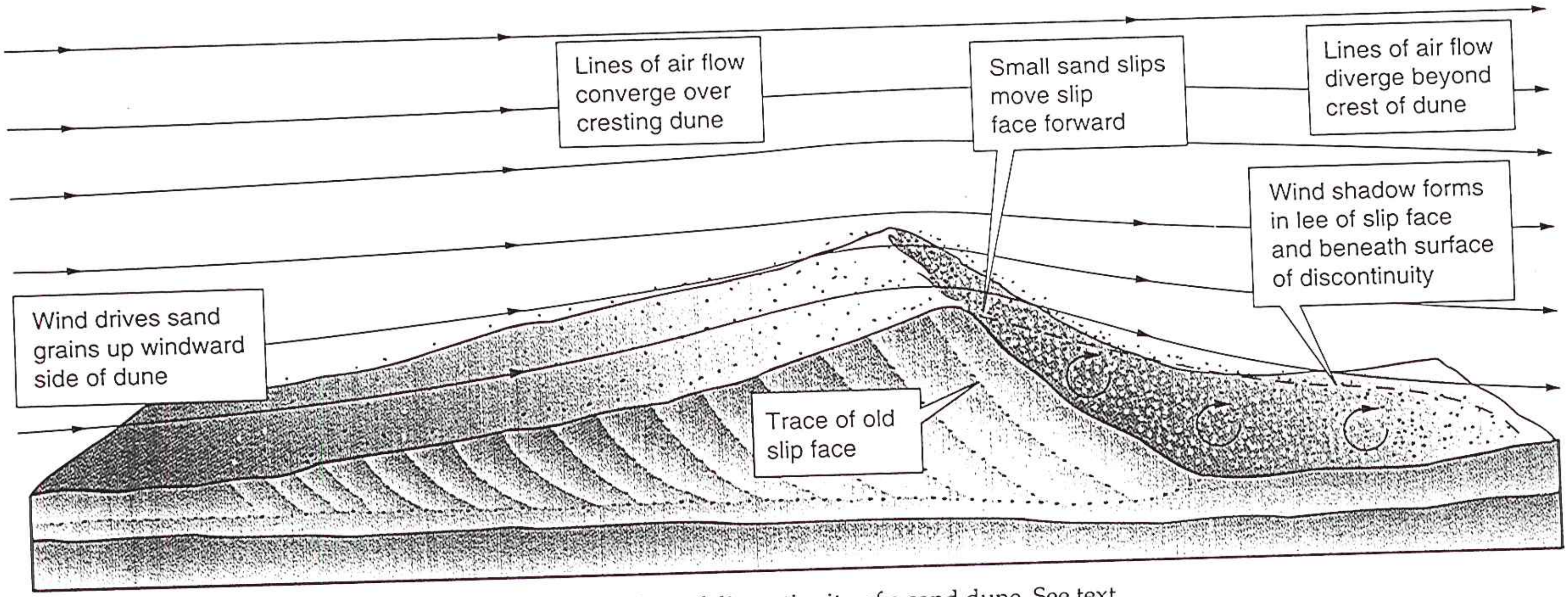

FIGURE 18.19 The wind shadow, slip face, and surface of discontinuity of a sand dune. See text for discussion.

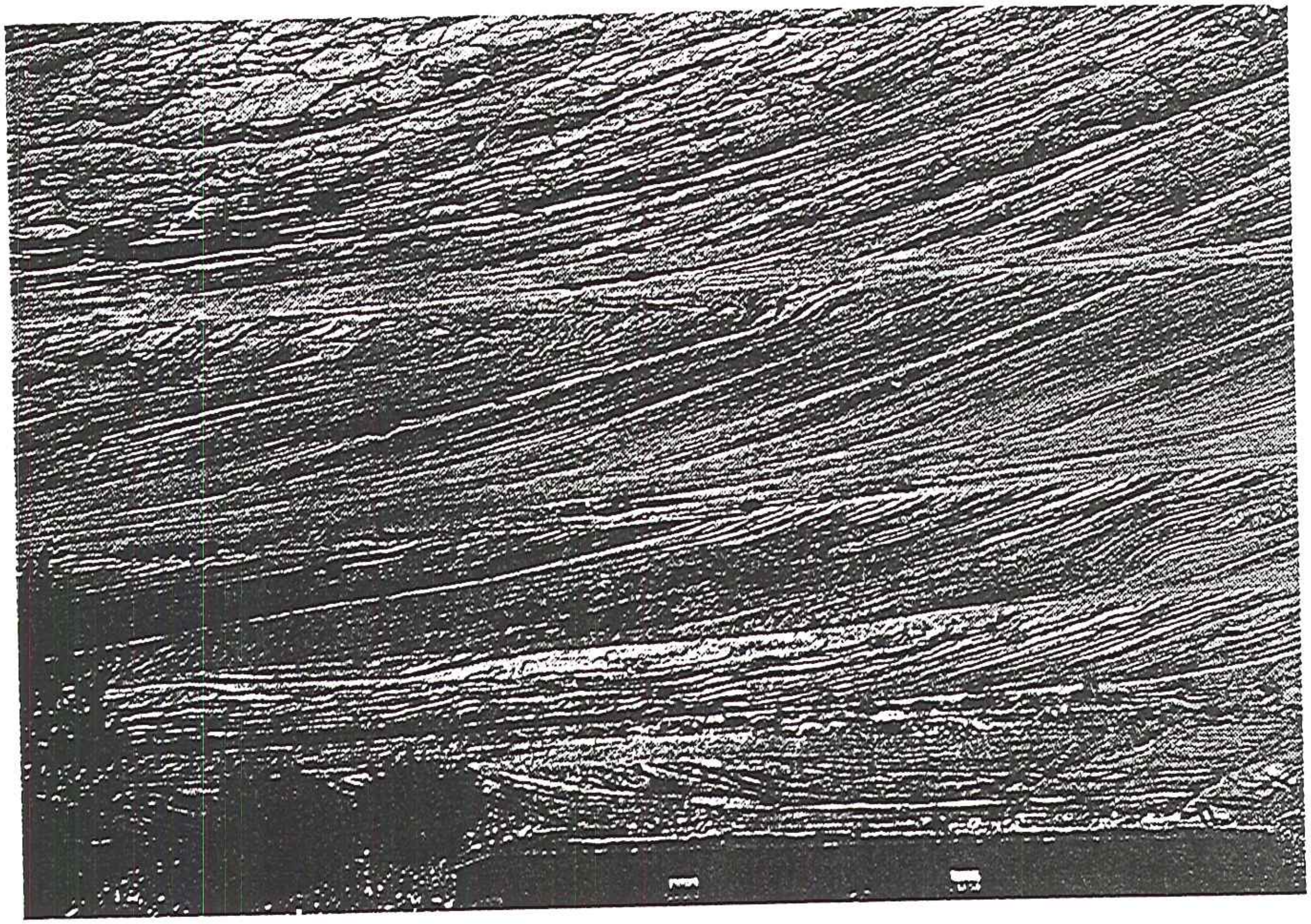

FIGURE 18.23 These inclined beds of ancient windblown sands are now lithified. The dipping beds record the slip faces of dunes in a Jurassic desert. Kanab Canyon, Utah.

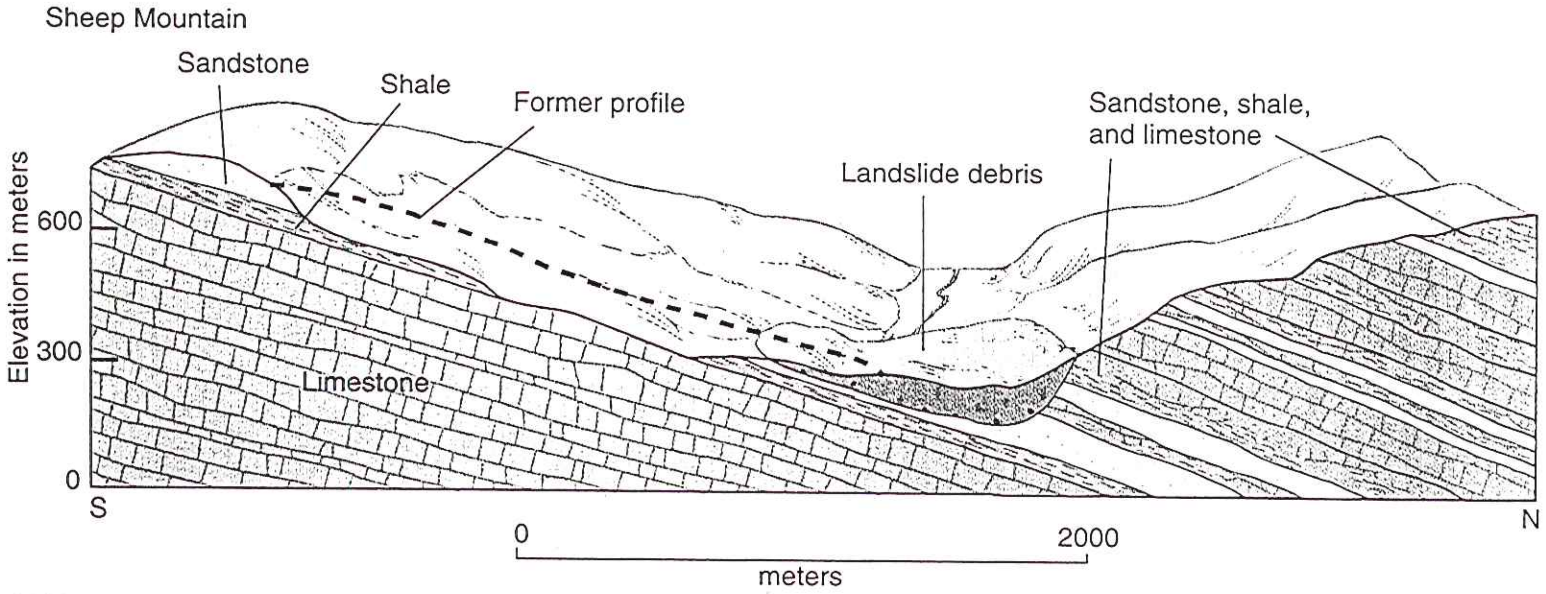

FIGURE 13.17 Diagram showing the nature of the Gros Ventre slide. Note that the sedimentary beds dip into the valley from the south. The large section of sandstone slid downward along the shale bed. *(Redrawn from William C. Alden, "Landslide and Flood at Gros Ventre, Wyoming,"* Trans. AIME, *Vol. 76, p. 348, 1928.)*

Cohesion is what supports cliff faces at angles > angle of repose

e.g.

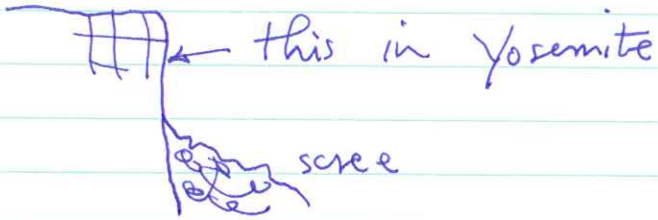

Much more variable — crudely, how easy to break by whang with a hammer.

For local Princeton rocks, which you have now whanged...

Brunswick shale : C ~ 5 MPa

Stockton sandstone : C ~ 15 MPa

Rocky Hill diabase : C ~ 100 MPa

Clay-rich rocks & fault zones : C $\lesssim$ 0.2 MPa

Sliding often occurs on weak layer in sedimentary sequences, e.g. Gros Ventre slide in text:

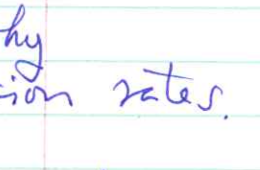

Weathering reduces cohesion — this is why it exerts a strong control on erosion rates.

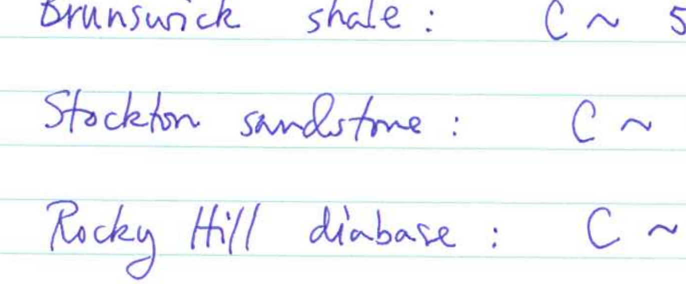

often it is the weathered layer that slides off in a landslide — exposes relatively unweathered rock beneath

Stability analysis for the Frank slide Alberta

Bedding plane slip in jointed limestone.

$\rho = 2700 \frac{kg}{m^3}$

Parameters : $\theta = 50^\circ$

$h = 150 \; m$

Cohesion needed to prevent sliding :

$$C = \rho g h \cos^2\theta \; (\tan\theta - \mu)$$

μ	Critical
0.6	1 MPa
0.85	0.5 MPa

The actual cohesion measured (after the slide) is shown in Table 1

$C \approx 0.2$ MPa

Could this catastrophe have been predicted ?

Fig. 14 shows that such bedding plane slides are quite common.

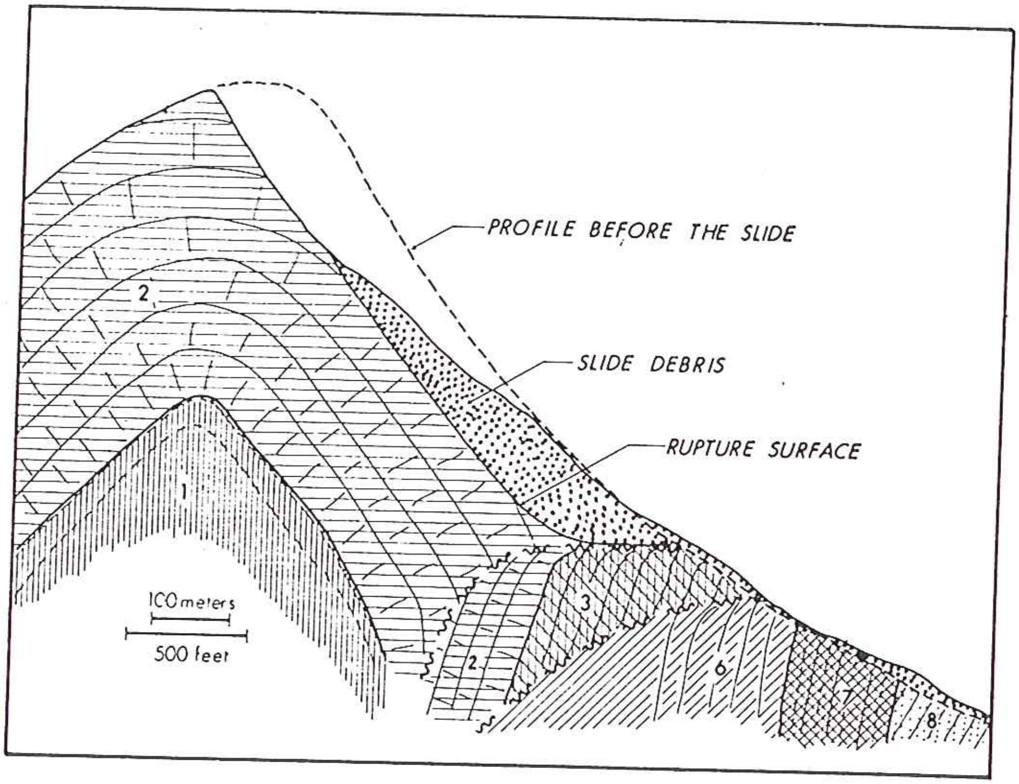

Fig. 8. Cross-section through Turtle Mountain along line $C—C'$ shown in Fig. 5. For legend, see Fig. 5.

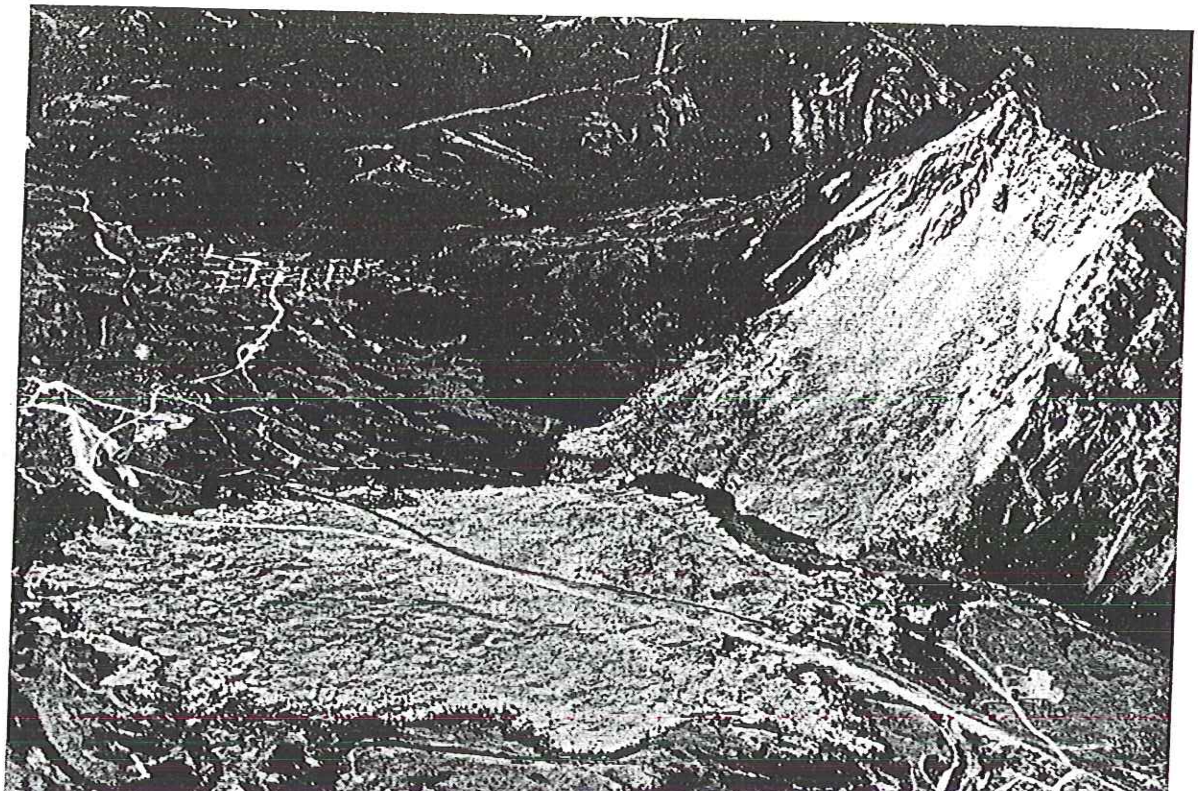

Fig. 9. Oblique aerial view of Frank slide from the northeast.

FRANK ROCKSLIDE, ALBERTA, CANADA

TABLE I

Summary of shear strength parameters

Type of sample	Peak		Ultimate	
	ϕ	$c(\mathrm{kN/m^2})$	ϕ	$c(\mathrm{kN/m^2})$
Bedding plane	51.7	262	32.3	55
Flexural-slip surface	28.0	221	15.6	124
Joints	32.0	172	14.0	83
Diamond-saw cut	29.0	0	29.0	0
Surface lapped with 45/80 grit	—	—	37.2	34.5

$C \approx 0.2-0.3$ MPa

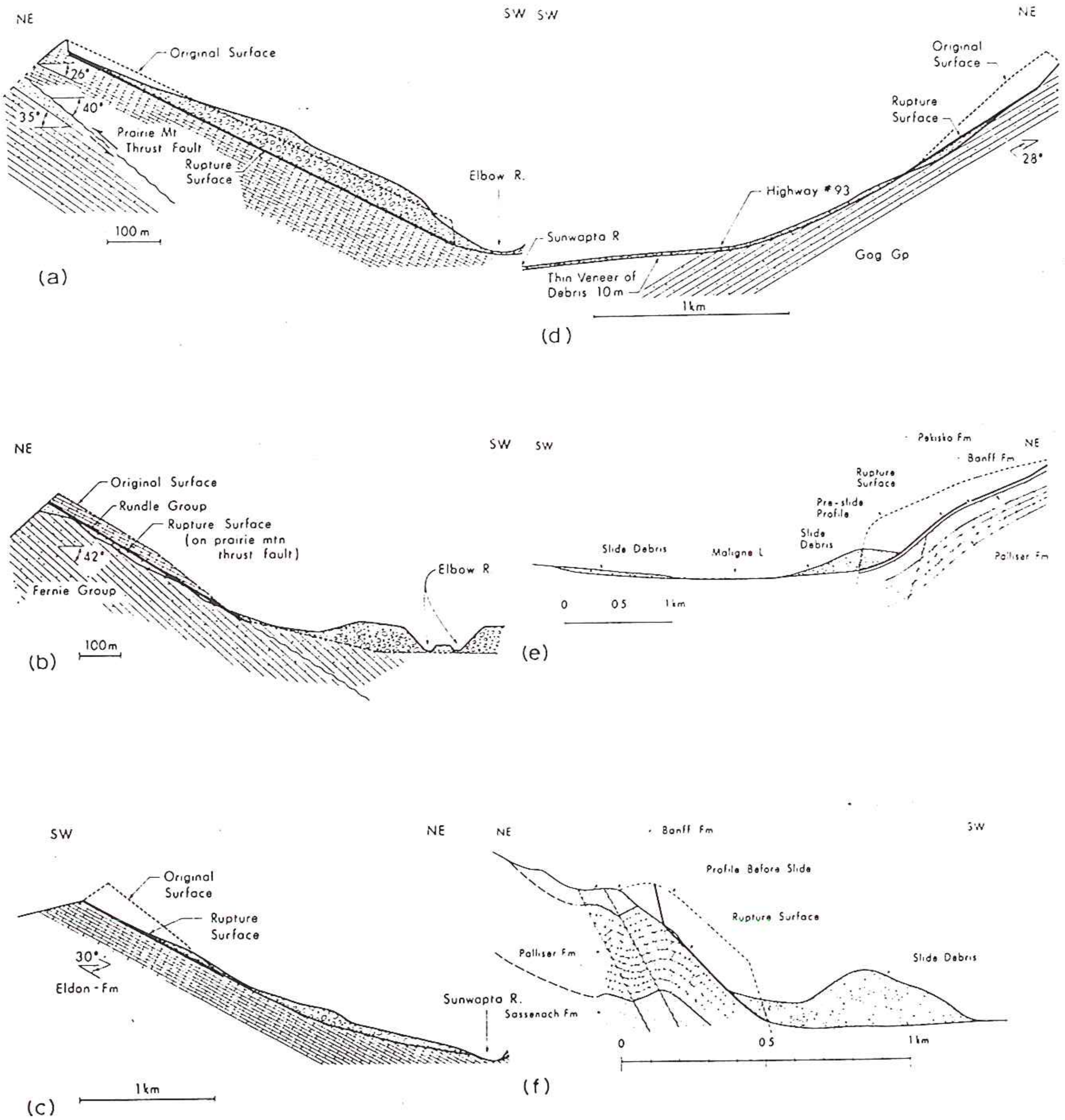

Fig. 14. Sections of major rockslides of the Canadian Rocky Mountains (after Cruden, 1976): (a) Beaver Flats north, (b) Beaver Flats south, (c) Mt. Kitchener, (d) Jonas Creek north, (e) Maligne Lake, (f) Medicine Lake. See Table II for data. Courtesy of the National Research Council of Canada.

Ground water also exerts a direct mechanical influence on slides (<u>Hubbert – Rubey</u> effect)

Analysis of <u>wet landslides</u>:

h_r : thickness of slide block

h_w : height of water table above slide surface

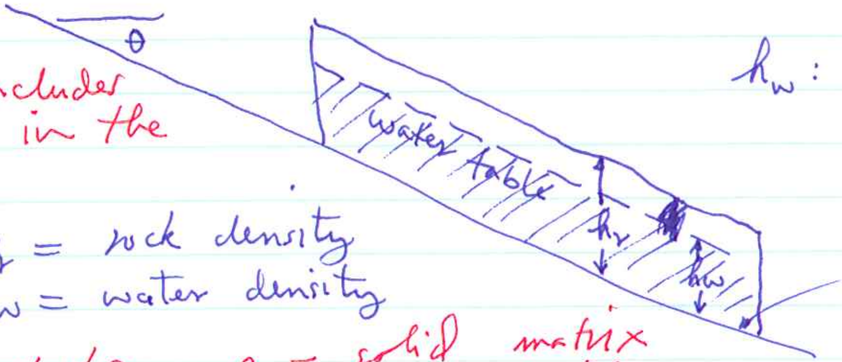

contact area 1 × 1 m²

note: ρ_r includes the water in the pores

ρ_r = rock density
ρ_w = water density

$\rho_r = (1-\phi)\rho_s + \phi\rho_w$, ρ_s = solid matrix density

The sliding force is unchanged:

$$F_{slide} = \underbrace{\rho_r g h_r \cos\theta}_{W} \sin\theta$$

But the effective normal force is reduced by the <u>buoyancy force</u> of the water:

Archimedes principle

$$N_{effective} = (\rho_r h_r - \rho_w h_w) g \cos^2\theta$$

$$W_{effective} = (\rho_r h_r - \rho_w h_w) g \cos\theta$$

$$F_{resist} = C + \mu N_{effective}$$

Ignoring cohesion ($C \simeq 0$) we find

$$\boxed{\tan\theta = \mu\left(1 - \frac{\rho_w h_w}{\rho_r h_r}\right) = \mu_{effective}}$$

The effective coefficient is reduced by this buoyancy effect [redacted]

[redacted]

μ	θ_{dry}	$\theta_{saturated}$ ($h_w = h_r$)
0.85	40°	27°
0.6	31°	20°
0.4	22°	13°
0.2	11°	7°

assumes $\rho_r = 2500$ kg/m^3

$\Rightarrow 1 - \frac{\rho_w}{\rho_r} = 0.6$

This effect can act to reduce the critical slope substantially — this is why large rainstorms frequently trigger slides.

e.g. Hurricane Mitch 1998

The effect can be even more pronounced when an impermeable clay layer traps fluids, leading to artesian conditions ($h_w > h_r$)

How would you inhibit landslides on a natural or man-made slope?

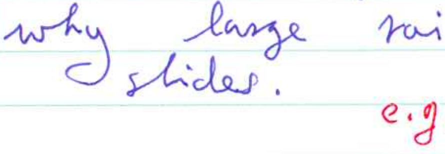

drainpipes to relieve pressure — or divert H_2O above to reduce infiltration

Do aluminum block demo at end of class — show not just a lubrication effect

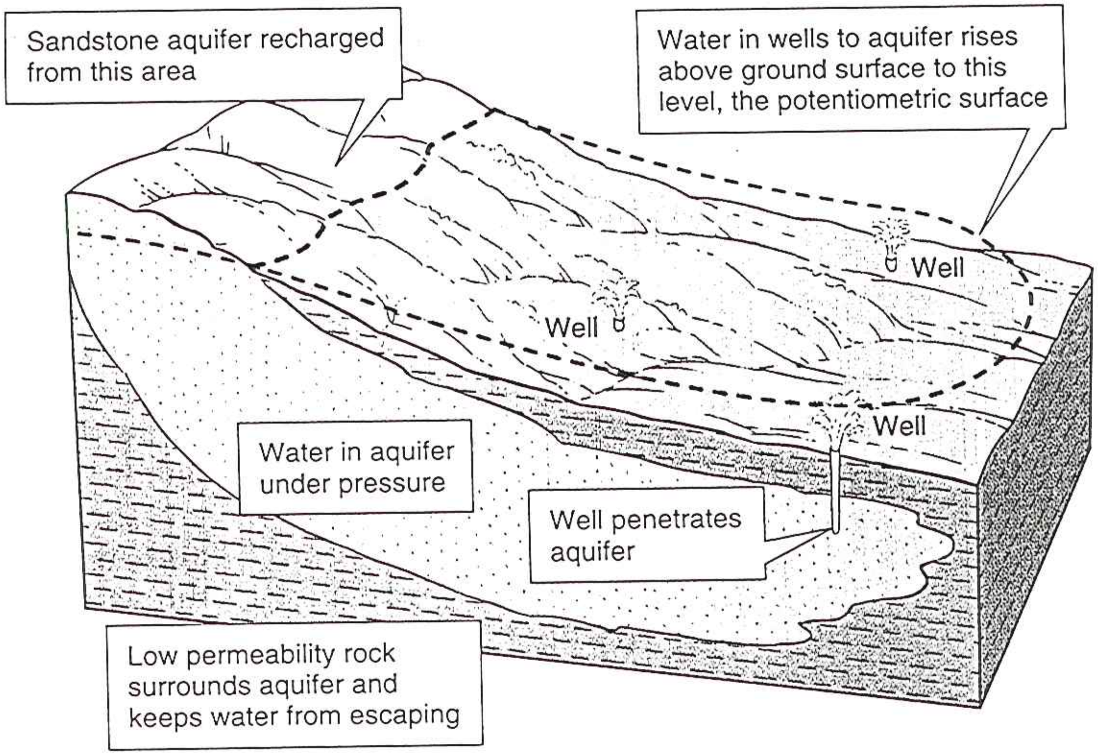

FIGURE 15.13
The wells in the diagram meet the conditions that characterize an artesian system: (1) an inclined aquifer, (2) confined by low permeability layers that prevent water from escaping vertically or laterally, and (3) sufficient pressure to force the water above the aquifer wherever it is tapped. Water in the wells shown rises to the level of the potentiometric surface.

Sediment flux from a mountain belt derived by landslide mapping

Niels Hovius*
Department of Earth Sciences, University of Oxford, Parks Road, Oxford OX1 3PR, United Kingdom
Colin P. Stark
Géosciences, Université de Rennes, Campus de Beaulieu, 35042 Rennes, France
Philip A. Allen*
Department of Earth Sciences, University of Oxford, Parks Road, Oxford OX1 3PR, United Kingdom

ABSTRACT

In humid uplands landsliding is the dominant mass wasting process. In the western Southern Alps of New Zealand landslides are scale invariant and have a power-law magnitude frequency distribution. Independent studies from other regions suggest that this is a general property of landsliding. This observation is of critical importance to the evaluation of the impact of events of different length scales over different time intervals on landscape evolution. It is particularly useful when estimating regional geomorphic rates, because it constrains the frequency and overall significance of extreme events, which cannot otherwise be evaluated. By integrating the complete response of the system, we estimate the regional denudation rate due to landsliding to be 9 ± 4 mm yr^{-1}. Sediment discharge from the western Southern Alps is dominated by landslide-derived material.

INTRODUCTION

Landscape evolution arises from the integrated effect of erosion and mass transfer over geologic spatial and temporal scales. In many humid uplands landscape evolution is dominated by landsliding across a wide range of length scales (Anderson, 1994; Gerrard, 1994; Greenbaum et al., 1995; Schmidt and Montgomery, 1995; Burbank et al., 1996). A great body of work documents the morphology and mechanics of individual instances of slope instability, but few studies have considered the process at a larger scale. Furthermore, direct observations of the long-term role of landsliding are lacking. Extrapolating short-term geomorphic observations to time scales pertinent to landscape development requires an understanding of the scaling behavior of the processes involved, in particular the magnitude and frequency with which they occur (Wolman and Miller, 1960). Magnitude-frequency studies require a broad range of spatial and temporal constraints and a large number of observations. These three conditions are met in the central section of the western Southern Alps of New Zealand, where we have obtained a 60 yr record of landsliding from multiple sets of air photos. This data set has enabled us to quantify the rates and scaling of landsliding and the concomitant mass fluxes.

STUDY REGION

The Southern Alps are a linear, asymmetric mountain belt marking the oblique compressional boundary between the Australian and the Pacific plate (Walcott, 1978). Rock uplift rates approaching 7 mm yr^{-1} (Bull and Cooper, 1986; Tippett and Kamp, 1993; Simpson et al., 1994) have assisted the building of 2 to 4 km of relief, which forms a barrier across the prevailing, moisture laden, northwest winds moving off the Tasman Sea. Mean annual precipitation rates reach as much as 15 m on the steep western flank of the orogen (Griffiths and McSaveney, 1983a). Here, dissected, rectilinear slopes, frequently steeper than 45° and with thin (<1 m) regolith cover, have formed in zones of schists and gneisses trending parallel to the range bounding Alpine fault. Dense, natural, temperate rain forests prevail below a tree line at ~1200 m altitude. These conditions are very favorable to the occurrence of rapid mass wasting. The principal hillslope erosion processes are landslides, involving falls, slumps and slides, predominantly displacing bedrock, and debris flows (definitions according to Varnes, 1978).

LANDSLIDE MAPPING

The availability of multiple sets of air photos for the central Southern Alps, for the period between 1948 and 1986, allows assessment of the distribution of landsliding both in space and time (Hovius, 1995). The study region is enclosed by the Waitaha River and the Moeraki River, the western coastline of South Island, and the main divide of the Southern Alps (Fig. 1). This region comprises 13 transverse catchments draining the central segment of the Southern Alps toward the west and their downstream continuation across a narrow coastal plain. Two series of air photos (1964/65, 1:16 500; 1985/86, 1:50 000) provide complete coverage of the study region. Additional coverage of the coastal plain and the frontal part of the mountain belt is available for the intermediate period (1972/73, 1:25 000; 1980/81, 1:25 000). For the area north of the Karangarua River time coverage includes the series of 1948 (1:15 840). In all, 2640 photos were inspected in a regional reconnaissance of highly inaccessible terrain. Approximate dates of erosional events were established by comparing photographic coverage made at intervals.

Recent landslides can be discerned on air photos using morphometric criteria and high surface reflectivity. Reflectivity contrasts between vegetated and nonvegetated zones fade as erosion scars are recolonized by vegetation, thus adding a distinction between recent and subrecent events. In the nival zone, where vegetation is absent, such discrimination is impossible. The present reconnaissance is therefore limited to the lower, vegetated parts of the mountain belt, below ~1400 m altitude.

All landslide scars and debris flows identified on the air photos were mapped on 1:50 000 scale topographic maps, where available, and on 1 in:1 mi maps for the remaining parts of the region (both map series: Department of Survey and Land Information, Wellington, New Zealand) and were subsequently digitized. As a rule, only scars or deposits without second-growth vegetation were included. In the remainder of this paper we discuss landslide scars only. The areas of individual landslides observed in the study region range from 100 m^2 to about 1 km^2. Mapping resolution was primarily determined by the scale of the maps; in this study it is reasonable to assume a maximum mapping accuracy of 1.5 mm, which is equivalent to 75 m on a 1:50 000 scale map. The effective mapping range therefore has a lower limit of 5×10^{-3} km^2. Simultaneous field-

---

*Present address: Department of Geology, Trinity College, Dublin 2, Ireland.

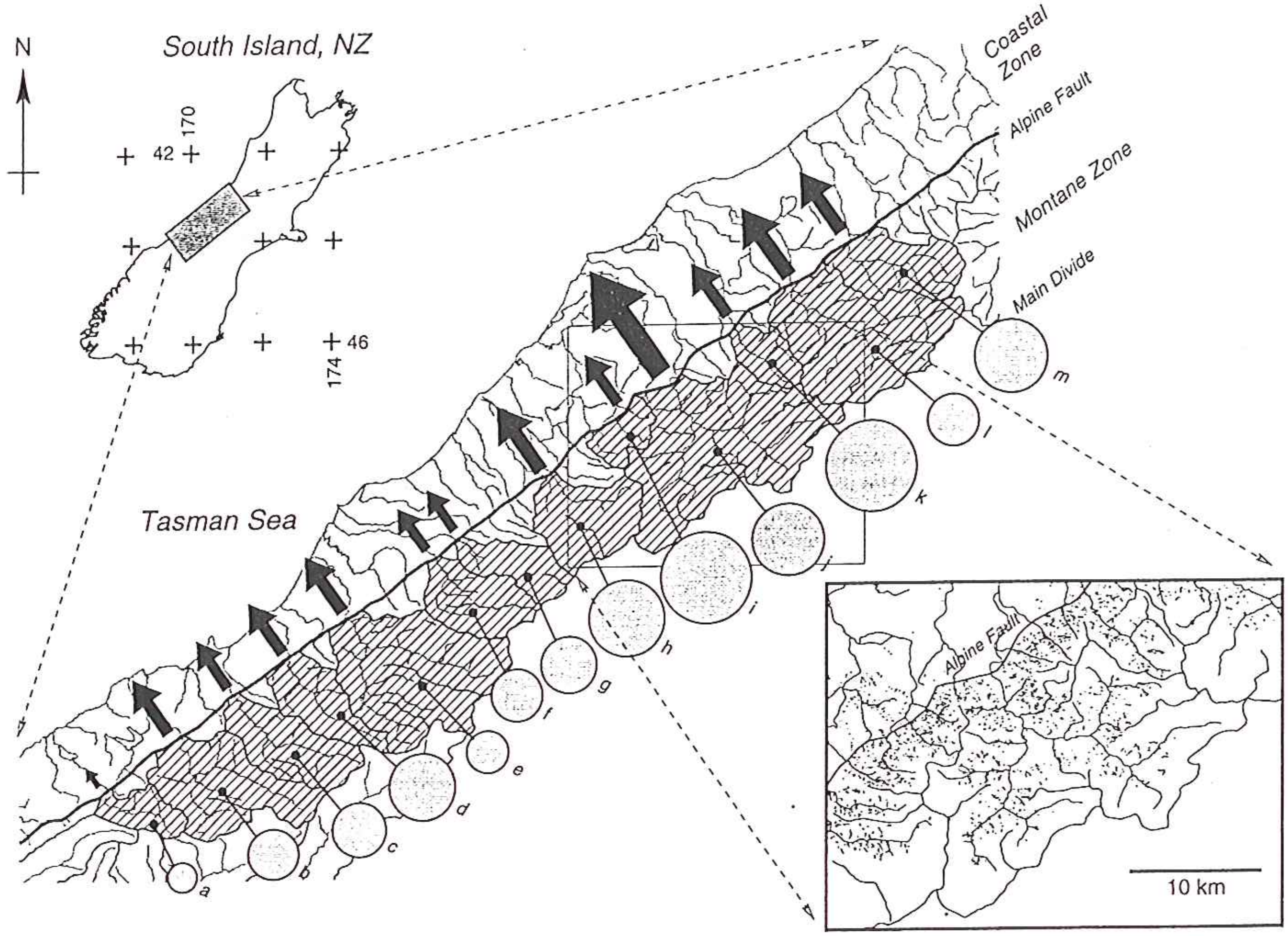

Figure 1. Overview of denudation rates and sediment discharges from 13 catchments draining western side of Southern Alps, calculated from 60 y. landslide record. Inset shows section of landslide data base, covering montane part of Whataroa catchment, flanked by Poerua and Waitangitaona basins. Denudation rates (E) and sediment discharges (D) are indicated respectively by circles and arrows, the areas of which are proportional tc each estimate, and are listed as follows: (a) Moeraki: E = 1.8 mm yr^{-1} (D = 1.2×10^5 m^3yr^{-1}); (b) Paringa: E = 5.5 mm yr^{-1} (D = 1.3×10^6 m^3yr^{-1}); (c) Mahitahi: E = 6.3 mm yr^{-1} (D = 9.8×10^5 m^3yr^{-1}); (d) Makawhio: E = 9.9 mm yr^{-1} (D = 1.1×10^6 m^3yr^{-1}); (e) Karangarua: E = 3.7 mm yr^{-1} (D = 1.3×10^6 m^3yr^{-1}) (f) Cook: E = 5.8 mm yr^{-1} (D = 7.9×10^5 m^3yr^{-1}); (g) Fox: E = 7.5 mm yr^{-1} (D = 7.1×10^5 m^3yr^{-1}); (h) Waiho: E = 12.2 mm yr^{-1} (D = 2.0×10^6 m^3yr^{-1}); (i) Waitangitaona: E = 18.1 mm yr^{-1} (D = 1.1×10^6 m^3yr^{-1}); (j) Whataroa: E = 11.4 mm yr^{-1} (D = 5.1×10^6 m^3yr^{-1}); (k) Poerua: E = 18.1 mm yr^{-1} (D = 1.2 : 10^6 m^3yr^{-1}); (l) Wanganui: E = 6.1 mm yr^{-1} (D = 2.1×10^6 m^3yr^{-1}); (m) Waitaha: E = 11.6 mm yr^{-1} (D = 1.7×10^6 m^3yr^{-1}).

work in several catchments in early 1994 validated the mapping technique. Most scars predating 1973 were overgrown with shrubs, whereas younger scars supported little second-growth vegetation. Thus the temporal resolution of the mapping method was found to be ~20 years.

Following the method we have outlined, we generated a map of the distribution of landslides on the western flank of the central Southern Alps and the adjacent coastal plain (Fig. 1). This region has a total surface area of 4970 km^2, 2670 km^2 of which are vegetated montane terrain and therefore mappable. In all, 7691 landslides were mapped, representing between 40 and 60 years of mass wasting, depending on the location.

Landslide density is clearly higher in the Alps or montane zone compared to the coastal zone, with an abrupt increase at the range bounding Alpine fault. Because the two zones have important topographic, climatologic, and geologic differences, their landslide inventories should not be combined. In this study we have therefore focused on the distribution of landslides in the montane zone.

MAGNITUDE AND FREQUENCY

The mapped areas of all 4984 observed landslides in the montane zone east of the Alpine fault exhibit a magnitude-frequency distribution (Fig. 2) that can be described by a power law over the approximately two orders of area magnitude for which reliable measurements are available. This distribution may be written in a cumulative form,

$$n_c(A \geq A_c) = \kappa (A_c/A_r)^{-\beta} A_r\,, \qquad (1)$$

where $n_c(A \geq A_c)$ is the number of slides per year of magnitude greater than or equal to A_c over a reference area A_r, κ is the rate of landsliding per unit area per year, and β is a dimensionless scaling exponent. We define A_r = 1 km^2, and obtain the best fit power law model (1) by linear regression over the restricted, but most robust, dat range from 10^{-2} km^2 to 10^{-1} km^2. As Figure : shows, the gradient of the log-log form of th model is β = 1.16, and the intercept at $A = A_r$ i $\kappa = 5.4 \times 10^{-5}$ km^{-2} yr^{-1}.

A similar scale-invariant distribution (Tur cotte, 1992) of landslide-magnitude frequenc has been observed by Fuyii (1969) in a sample o about 650 rainfall-induced events from uplan areas of Japan. For magnitudes ranging betwee 10^{-3} km^2 and 10^{-1} km^2, Fuyii found that β = 0.9 Sugai et al. (1994) conducted a more extensiv study in the Akaishi Mountains of central Japa Rather than considering the magnitude of land slide scars, they measured the area of individu landslide deposits, discarding all observation smaller than 10^{-2} km^2. Their results indicate power law distribution of landslide-magnitud frequency over an area scale range of less tha one order of magnitude, with a regional value c β of ~1.0. Given independent observations c power law scaling behavior from three regions, it seems that scale invariance is a general property of landslides, although differences exist between fitted model parameters.

VOLUMETRIC ANALYSIS

In order to estimate the total volume of material eroded by landsliding we need to quantify the geometry of the landslides as well as their size distribution. We have found the mean plan form of Southern Alps landslides to be approximately elliptical with an aspect ratio of about 2.0 across all length scales. As the inset in Figure 2 shows, the minor axis length (width) of the landslide is roughly equal to the square root of its area, $l \approx \sqrt{A}$, so that we can rewrite equation 1 using this width measure:

$$n_c(l \geq l_c) = \kappa l_c^{-2\beta}. \tag{2}$$

Landslide width, rather than length, is chosen as the equivalent length scale because its relationships with respect to both landslide area and thickness are more tightly constrained in our data set. Field studies (Ohmori, 1992; Hovius, 1995) suggest a linear width-depth scaling relation for mean slide thickness t:

$$t(l) = \varepsilon l. \tag{3}$$

Cross sections of several larger landslide scars in the montane area yield an estimate for ε of 0.05 ± .02. The landslide volume discharge at length scale l is therefore given by

$$v(l) = n(l)A(l)t(l) = \varepsilon l^3 n(l), \tag{4}$$

where $n(l)$ is the number distribution of landslides of length l, derived from the cumulative distribution of equation 2 by $n(l) = \mathrm{d}n_c / \mathrm{d}l$. The total volume of landslide material yielded from the reference area A_r is then

$$V = 2\beta\varepsilon\kappa \int_{L_0}^{L_1} l^{2-2\beta} \mathrm{d}l, \tag{5}$$

where L_1 is the maximum possible width of a landslide in the region and L_0 is the minimum. From this follows the very important conclusion that when $\beta < 1.5$ and $L_1 >> L_0$, as is the case in the Southern Alps, denudation due to landsliding is dominated by the largest events. Then we obtain

$$V \approx \frac{2\beta\varepsilon\kappa}{(3-2\beta)} L_1^{3-2\beta} \tag{6}$$

The upper length scale for landsliding in the region, L_1, is not precisely determined. The largest observed event has a width of ~1 km and an area of 1 km², but the dimensions of the longest valley sides would allow for the occurrence of events of well over 2 km. Because no relicts of such larger events have been identified in the postglacial landscape, we consider $L_1 \approx 1$ km. Using $\kappa = 5.4 \times 10^{-5}$ km^{-2} yr^{-1} for the 2670 km² mapped montane zone, we obtain an estimate for the denudation rate due to landsliding of the western Southern Alps of 9 ± 4 mm yr^{-1}.

Assuming that the observed scaling behavior is a general characteristic of landslides throughout the region, local landsliding rates may be determined using data from each catchment over the size range of 10^{-2} km² to 10^{-1} km², for which equation 1 produces the most robust fit. Using equation 6, these local values of κ were converted into estimates of denudation rate, shown as circles in Figure 1. Most drainage basins were found to have denudation rates between 5 mm yr^{-1} and 12 mm yr^{-1}, although higher rates were observed in two small basins at the range front. These denudation rates were then integrated over the surface area of each catchment to obtain local annual sediment discharges, shown as arrows in Figure 1. Discharges range from 1 × 10^6 m³yr^{-1} to 2 × 10^6 m³yr^{-1}, with a peak value of 5 × 10^6 m³yr^{-1} for the Whataroa catchment. These simple estimates are open to refinement, by a more sophisticated length-depth scaling relation for slides, and by a more precise definition of the maximum length scale on which sliding can occur. However, the relative proportions of catchment-wide denudation rates and sediment discharges will remain unaffected because both these factors are likely to vary little between drainage basins. An added requirement for extrapolation of denudation estimates beyond the period covered by the airphoto record is a well constrained relation between the rate of landsliding and the probability distribution of climatic and seismic triggers.

Denudation estimates may be compared with rates calculated from sediment discharge measurements for some streams along the Alpine fault, which range from 4.7 to 11.9 mm yr^{-1}. The two principal rivers in the region, the Hokitika to the north, and Haast to the south of the study region, have basin-wide denudation rates of 6.3 and 4.7 mm yr^{-1}, respectively (calculated from specific sediment yields listed in Griffiths, 1979). Denudation rates in the Waitangitaona catchment were estimated by Griffiths and McSaveney (1986) to be 4.6 ± 0.3 mm yr^{-1}, from a 17 yr deposition record on the alluvial fan at the range front. Measurements from Ivory basin, a partially glaciated cirque basin in the upper part of the Waitaha basin, give a five year average denudation rate of 5.5 ± 0.3 mm yr^{-1} (Hicks et al., 1990). In the nearby nonglaciated Cropp basin a three-year study (Griffiths and McSaveney, 1983b) yielded a denudation rate of 11.0 ± 0.9 mm yr^{-1}. As there is little intramontane storage of eroded

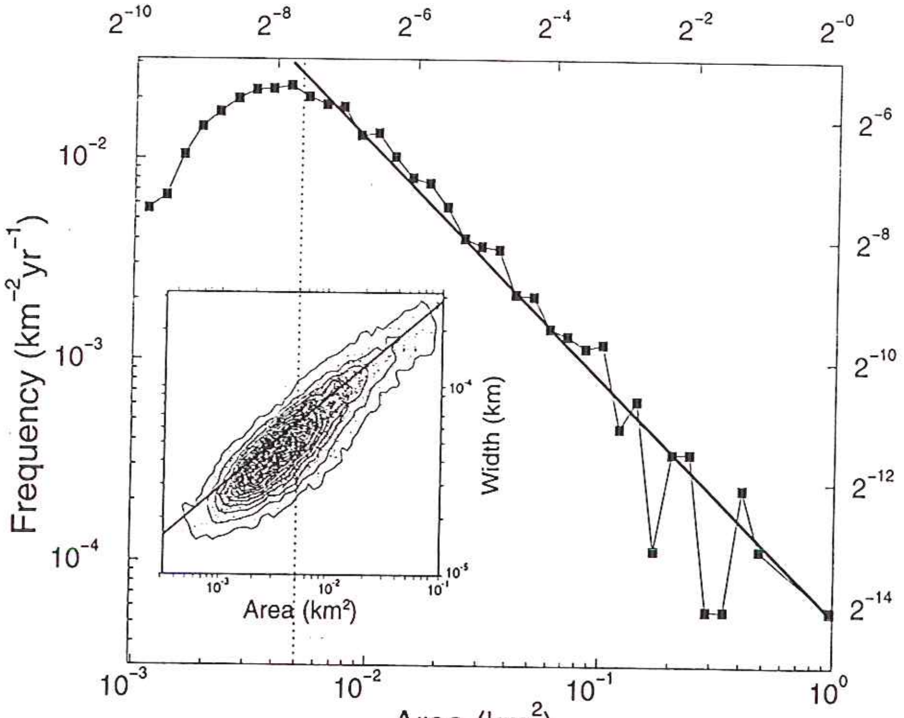

Figure 2. Size distribution of mapped landslides in central western Southern Alps. Main graph is histogram employing logarithmic bin widths (log 2w = 1/4). Mapping method puts lower bound of reliable frequency estimates at about 5 × 10^{-3} km², which is indicated (for both graphs) by vertical dashed line. Above this cutoff, very clear power law trend is observable over two orders of length scale magnitude. Straight line indicates best fit power law model, where gradient is equal to exponent β in equation 1. Correctly normalized, this curve describes probability density function of landsliding of certain magnitude at given time. Inset graph illustrates relationship between landslide area and width of best fit ellipse. This relation is employed in volumetric analysis (equations 3–6). Kink in histogram may be mapping artifact or reflection of size discontinuity in mass wasting mechanics.

Slope Transport
Landslides, soil slides, rock slides, rock avalanches

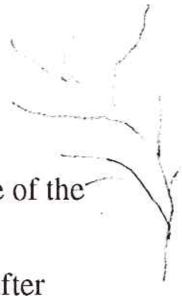

0. How does rock/sediment get into streams to be transported?? Most of the surface of the land is not streams. How does soil and rock get into streams? Manyways:

slope wash, rills----most important for exposed soil, plowed fields, slopes after
    fires, fresh unvegitated volcanic ash, etc
    (note in many cases these are human effects)

"Overland Flow"
"headward Erosion of channels"

mass movement of slopes
- rock fall
- rock and slides
- rock avalanches (airborne)
- landslides (soil slides)
- rock and soil flow
- soil creep (solifluction)

mass movement may be the most important mechanism of slope transport

I. frictional sliding of a block down an inclined plane

Amonton's laws of friction

[i] Friction proportional to normal force

$$F = \mu W \sin \theta$$

$$\tan \theta = \mu_f (1 - \lambda_f)$$

[ii] Friction is independent of area of contact!!!

Typical coefficients of friction

typical coefficients of friction generally independent of rock type at crustal (tectonic conditions)

Some exceptions: salt, graphite, smectite? probably non-frictional behavior (crystalline plasticity, i.e. metamorphic flow)

Critical slope for sliding

The problem of slides down gentle slopes
- Example of Hart Mtn.
- Examples of Palos Verdes

I'. Effect of cohesive strength

II. Sliding in the Rain

Effect of water on the sliding angle

Effect of water on the sliding of soil

III. Impermiable clay layers & excess fluid pressures

Causes of "abnormal" fluid pressures (in excess of hydrostatic)
- [1] artesian head
- [2] sudden loading of impermeable clay

Transient high pressure in response to load

Example of the earth-fill dam

How would you inhibit landslides on a natural or man-made slope?

put drainage pipes in hillside
limit uphill water infiltration

III. How does weathering and soil formation promote landslides?

- [1] weathering breaks down the cohesion of the rock
- [2] some clays appear to have a low coefficient of friction
- [3] clay seal may promote artesian excess pressure

V. Bedrock down-dip slides

Palos Verdes
Frank
Gros Vent
Iranian slide
Hart Mtn. Slide
Spanish Pyrenees example

VI. airborne avalanches

VII. mud/debris flows

VIII. soil creep

IX. Particulate erosion on slopes